Hindawi
Advances in Civil Engineering
Volume 2019, Article ID 8052413, 14 pages
https://doi.org/10.1155/2019/8052413

Research Article

Estimation of Additional Equivalent Damping Ratio of the Damped Structure Based on Energy Dissipation

Xiuyan Hu, Qingjun Chen, Dagen Weng, Ruifu Zhang, and Xiaosong Ren

Department of Disaster Mitigation for Structures, Tongji University, Shanghai 200092, China

Correspondence should be addressed to Xiaosong Ren; rxs@tongji.edu.cn

Received 25 April 2019; Revised 28 June 2019; Accepted 25 July 2019; Published 15 August 2019

Academic Editor: Cristiano Loss

In the design of damped structures, the additional equivalent damping ratio (EDR) is an important factor in the evaluation of the energy dissipation effect. However, previous additional EDR estimation methods are complicated and not easy to be applied in practical engineering. Therefore, in this study, a method based on energy dissipation is developed to simplify the estimation of the additional EDR. First, an energy governing equation is established to calculate the structural energy dissipation. By means of dynamic analysis, the ratio of the energy consumed by dampers to that consumed by structural inherent damping is obtained under external excitation. Because the energy dissipation capacity of the installed dampers is reflected by the additional EDR, the abovementioned ratio can be used to estimate the additional EDR of the damped structure. Energy dissipation varies with time, which indicates that the ratio is related to the duration of ground motion. Hence, the energy dissipation during the most intensive period in the entire seismic motion duration is used to calculate the additional EDR. Accordingly, the procedure of the proposed method is presented. The feasibility of this method is verified by using a single-degree-of-freedom system. Then, a benchmark structure with dampers is adopted to illustrate the usefulness of this method in practical engineering applications. In conclusion, the proposed method is not only explicit in the theoretical concept and convenient in application but also reflects the time-varying characteristic of additional EDR, which possesses the value in practical engineering.

1. Introduction

Energy dissipation technology, which has been used in civil engineering for decades, has proven to be an effective tool to resist earthquakes [1, 2]. Through the balanced installation of dampers in a structure, a large amount of seismic energy can be consumed, thereby protecting the structure from the effects of severe earthquakes [3, 4]. As a commonly used form of seismic technology, energy dissipation devices have been widely studied and extensively developed. Various types of dampers based on different energy-consuming mechanics have been proposed and used in engineering practice worldwide [4–8].

In many research studies and in engineering practice, it has been found that the mitigation effects of the seismic response resulting from the installation of dampers can be evaluated according to the additional equivalent damping ratio (EDR) [9, 10]. Moreover, researches show that the energy dissipation capacity of dampers can be reflected by the additional EDR [11, 12]. The additional EDR can connect the mitigation effects of the seismic responses to the energy dissipation capacity of dampers, which may simplify the procedure of retrofit design of structures. In this manner, the common methods used for designing damped structures are related to the required damping ratio [13–17]. Based on the required damping ratio, the parameters of the dampers are determined. On the basis of the abovementioned reasons, it is obvious that the additional EDR obtained from the installed dampers is an important factor in the design procedure of damped structures. The EDR is a basic concept in structural dynamics, and there are some classical methods to estimate the EDR of the structure, such as the free decay oscillation method and the half-power bandwidth method. The half-power bandwidth method is verified to be inaccurate to estimate the EDR of the structure in some cases, which

needs some corrections [18, 19]. The most common method is the strain energy method, which is expressed as follows [20]:

$$\xi_{\mathrm{eq}} = \frac{1}{4\pi} \cdot \frac{E_{\mathrm{D}}}{E_{\mathrm{So}}}, \tag{1}$$

where ξ_{eq} is the EDR, E_{D} is the energy dissipated by the system in one cycle, and E_{So} is the maximum strain energy in one cycle. The strain energy method is employed in many design codes [21, 22]. However, the method is accurate only when the system is in resonance. In addition, the method has some deficiencies in practical applications, such as complexity in calculating energy dissipation.

Because a large variety of dampers are available, the estimation of the additional EDR is not easy. Nevertheless, because of the importance of the additional EDR, many studies have been dedicated to the estimation of this parameter. Lee et al. [23] utilized the modal energy-formed Lyapunov function to obtain a closed-form solution for the additional EDR. Two-dimensional shear buildings with various kinds of dampers were introduced to verify the accuracy of the solution. Occhiuzzi [24] proposed a method based on the state-space representation of a dynamical system to calculate the modal damping ratio. This method was adopted to estimate the additional EDR of structures with dampers that were configured by some existing design methods. The results showed that these damped structures yielded a similar additional EDR, which was approximately 0.2. Diotallevi et al. [25] defined a damping index and presented a method to directly estimate the EDR using the index. Iterations were not needed in the method, which was verified using a single-degree-of-freedom (SDOF) system. Park [26] investigated the damping of an inelastic SDOF system with an added damper. Damping correction factors and regression equations were utilized to estimate the additional EDR. Guerrero et al. [27] proposed an experimental approach to measure the damping of the structures with buckling-restrained braces (BRBs). The approach was verified by the shaking table tests, and the results showed that the energy dissipation of BRBs must be considered in the seismic design of the structure. Papagiannopoulos and Beskos [28] developed a modal damping identification model to estimate the modal damping ratios of the structures. This method was utilized by Katsimpini et al. [29] to obtain the modal damping ratios of the structure with the seesaw system, and the results indicated that the seesaw system could provide significant damping capacity. Li et al. [30] determined the damping in an SDOF system with a Maxwell damper. By adopting the properties of the structure in free vibration, they obtained derivations for the first- and second-order equivalent damping.

The abovementioned researches indicate that the additional EDR can be accurately calculated by many methods, but these methods are generally complicated and not convenient for practical application. For practical application, the easiness of the method in understanding and application is as important as the accuracy. Therefore, it is necessary to put forward an approach that is easy to understand, convenient to apply, and accurate to estimate the additional EDR of damped structures.

In this study, based on the energy dissipation through structural inherent damping and through the use of dampers, a simple method is developed to estimate the additional EDR induced by the dampers. Compared to the strain energy method, the proposed method is more accurate and the concept is explicit and intuitive, which is also convenient for practitioners to apply. First, the energy governing equation of the system is established. According to the definition of the EDR in structural dynamics [20], the relationship between energy dissipation and the EDR is established, which indicates that the additional EDR reflects the energy dissipation capacity of dampers. In this manner, the ratio of the energy dissipated by structural inherent damping to that dissipated by dampers is utilized to estimate the additional EDR. After that, the determination of the calculation time for the energy dissipation is discussed. The result of energy dissipation can be obtained by the structural energy governing equation. Within the range of significant duration of the ground motion, energy dissipation can be calculated by the integrals of the damping forces of the primary structure and the dampers with respect to the corresponding displacements, respectively, of which the calculation can be completed programmatically or by the structural analysis program. Next, the procedure of the proposed method is presented. In addition, the feasibility of this method is verified by using an SDOF system with an added viscous damper. A six-story concrete benchmark model with metallic yielding dampers (MYDs) is introduced to illustrate the usefulness of this method in practical engineering applications. Finally, the accuracy of results obtained by the proposed method is shown by conducting a comparison study.

2. Method Based on Energy Dissipation

2.1. Establishment of Energy Governing Equation. The simplified model of an SDOF system with an added viscous damper is shown in Figure 1, where the viscous damper is simulated by the Maxwell model. According to structural dynamics, the differential equation of movement subjected to a horizontal earthquake can be written as follows [31]:

$$m\ddot{x} + c\dot{x} + f_{\mathrm{s}}(x, \dot{x}) + f_{\mathrm{d}}(x, \dot{x}) = -m\ddot{x}_{\mathrm{g}}, \tag{2}$$

where x, $\dot{x}$, and $\ddot{x}$ are the relative displacement, velocity, and acceleration of the mass, respectively; $\ddot{x}_{\mathrm{g}}$ is the ground acceleration; m is the mass; k is the stiffness of the system; c is the inherent damping coefficient of the system; $f_{\mathrm{s}}(x, \dot{x})$ is the elastic or inelastic resisting force of the system; and $f_{\mathrm{d}}(x, \dot{x})$ is the damping force of the damper. In the Maxwell model, k_{a} is the dynamic stiffness of the damper and c_{a} is the damping coefficient of the damper.

By integrating x in equation (2) in the range of the earthquake duration $[0, t]$, the energy response equation can be obtained:

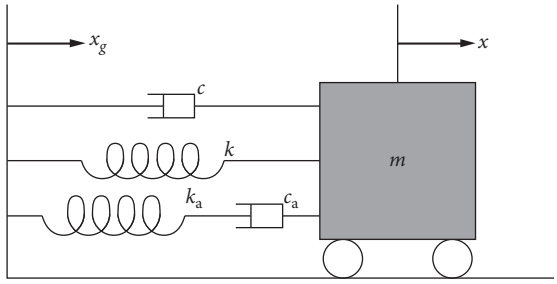

Figure 1: SDOF system with the damper.

$$m\int_0^t \ddot{x}\,dx + c\int_0^t \dot{x}\,dx + \int_0^t f_s dx + \int_0^t f_d dx = -m\int_0^t \ddot{x}_g dx. \tag{3}$$

Equation (3) can be rewritten as equation (4) in terms of energy:

$$E_k + E_c + E_h + E_e + E_d = E_{in}, \tag{4}$$

where E_k is the kinetic energy, E_c is the energy dissipated by the inherent damping of the primary structure, and E_h and E_e are the hysteretic energy and elastic strain energy of the primary structure, respectively. Here, $E_h + E_e = \int_0^t f_s \dot{x} dt$; when the primary structure is in an elastic state, $E_h = 0$. E_d is the energy dissipated by the dampers, and E_{in} is the energy input by ground motion.

2.2. Calculation of Additional EDR. In general, the energy dissipation capacity of the primary structure is indicated in terms of the EDR. Similarly, the energy dissipation capacity of additional devices can be indicated in terms of the additional EDR ξ_{eq}. According to the classic definition method for the additional EDR, the energy dissipated by the dampers is equalized with that dissipated by an equivalent viscous system during one vibration cycle [20]:

$$E_d = \int_0^{2\pi/\omega} f_d \dot{x}\,dt = \pi x_0^2 \omega c_{eq} = 2\pi\xi_{eq} k x_0^2 \left(\frac{\omega}{\omega_n}\right), \tag{5}$$

where ω is the circular frequency of excitation, x_0 is the maximum displacement of the structure in one cycle, c_{eq} is the equivalent damping coefficient of the dampers in one cycle ($c_{eq} = 2k\xi_{eq}/\omega_n$), and ω_n is the natural circular frequency of the structure.

This definition can be used to rewrite the equation for the additional EDR provided by the dampers during $[0, t]$ as follows:

$$E_d(t) = \int_0^t f_d \dot{x}\,dt = \int_0^t c_{eq}\dot{x}^2 dt = \frac{2\overline{\xi}_a k}{\omega_n}\int_0^t \dot{x}^2 dt, \tag{6}$$

where $\overline{\xi}_a$ denotes the additional EDR provided by the dampers in the seismic duration $[0, t]$ and t denotes the duration of the seismic record.

Meanwhile, the energy dissipated by the inherent damping of the primary structure can be expressed as follows:

$$E_c(t) = \int_0^t c\dot{x}^2 dt = \frac{2\xi_0 k}{\omega_n}\int_0^t \dot{x}^2 dt, \tag{7}$$

where ξ_0 denotes the inherent damping ratio of the primary structure.

From equations (6) and (7), the additional EDR of the dampers in the duration $[0, t]$ can be obtained:

$$\overline{\xi}_a(t) = \xi_0 \frac{E_d}{E_c} = \xi_0 \frac{\int_0^t f_d \dot{x}\,dt}{\int_0^t c\dot{x}^2 dt}. \tag{8}$$

It is obvious that the additional EDR $\overline{\xi}_a$ can be obtained from the inherent damping ratio and the ratio of the energy dissipated by the dampers to that dissipated by the inherent damping during $[0, t]$. It should be noted that the method focuses on the amount of energy dissipated and the manner to dissipate energy is not involved, which indicates that the method can be applied to various kinds of dampers. Equation (8) provides the expression for calculating the energy dissipation. When the damping force of the dampers and the inherent damping coefficient are known, the energy dissipation can be calculated by obtaining the integrals of the energy in equation (8).

By assuming that the additional EDR provided by the dampers is uniform throughout all the stories, i.e., $\overline{\xi}_{ai} = \overline{\xi}_a$, where $\overline{\xi}_{ai}$ is the additional EDR of the i-th story, and the vibration of the structure is dominated by the 1st mode, equation (8) can be applied in the multi-degree-of-freedom (MDOF) system. The energy dissipated by the dampers at i-th story E_{di} is

$$E_{di} = \sum_{j=1}^{m}\int_0^t f_{dj}\dot{x}_i dt = \frac{2\overline{\xi}_{ai}k_i}{\omega_1}\int_0^t \dot{x}_i^2 dt = \frac{2\overline{\xi}_a k_i}{\omega_1}\int_0^t \dot{x}_i^2 dt, \tag{9}$$

where f_{dj} denotes the damping force of the j-th damper at i-th story, m denotes the number of dampers installed at i-th story, $\dot{x}_i$ denotes the relative velocity between i-th and (i-1)-th story, and k_i denotes the stiffness of i-th story. And the energy dissipated by the inherent damping at the i-th story E_{ci} is

$$E_{ci} = \int_0^t c_i \dot{x}_i^2 dt = \frac{2\xi_0 k_i}{\omega_1}\int_0^t \dot{x}_i^2 dt, \tag{10}$$

where c_i is the damping coefficient of the i-th story. The ratio of energy dissipated by the dampers and the inherent damping of all the stories can be

$$\frac{E_d}{E_c} = \frac{\sum_{i=1}^{n_1} E_{di}}{\sum_{i=1}^{n} E_{ci}} = \frac{\sum_{i=1}^{n_1}\sum_{j=1}^{m}\int_0^t f_{dj,i}\dot{x}_i dt}{\sum_{i=1}^{n}\int_0^t c_i\dot{x}_i^2 dt} = \frac{(2\overline{\xi}_a/\omega_1)\sum_{i=1}^{n} k_i\int_0^t \dot{x}_i^2 dt}{(2\xi_0/\omega_1)\sum_{i=1}^{n} k_i\int_0^t \dot{x}_i^2 dt} = \frac{\overline{\xi}_a}{\xi_0}, \tag{11}$$

where $f_{dj,i}$ is the j-th damper installed at the i-th story, n_1 is the number of stories installed with dampers, and n is the number of stories.

The additional EDR of the structure $\overline{\xi}_{\mathrm{a}}$ can be obtained by rewriting equation (11) as follows:

$$\overline{\xi}_{\mathrm{a}}(t) = \xi_0 \frac{\sum_{i=1}^{n_1}\sum_{j=1}^{m}\int_0^t f_{\mathrm{d}j,i}\dot{x}_i dt}{\sum_{i=1}^{n}\int_0^t c_i \dot{x}_i^2 dt}. \tag{12}$$

Generally, as the dampers are not configured uniformly throughout all the stories, $\overline{\xi}_{\mathrm{a}}(t)$ denotes the average additional EDR of the entire structure in the duration $[0, t]$.

2.3. Determination of Calculation Time. In equation (8), the additional EDR of the dampers $\overline{\xi}_{\mathrm{a}}$ is a function of the seismic duration. An earthquake is a random vibration process. The seismic response varies with time, and the additional EDR depends on the seismic response [31]. Therefore, the additional EDR $\overline{\xi}_{\mathrm{a}}$ varies with time during the entire duration $[0, t]$. To reflect the energy dissipation capacity of the installed dampers during the most intensive period in the entire seismic motion duration, the calculation time should be determined. Generally, the dampers can ensure the maximum utilization of the energy dissipation capacity under large deformation, and large structural responses can be induced by intensive ground motion. Therefore, the time range covering the most intensive seismic motion can be adopted as the calculation time for the energy dissipation.

Significant duration parameters are generally utilized to describe the duration characteristic of the ground motion recorders [32]. The significant duration is defined as the time intervals in which a specified amount of energy is dissipated. The integral of the square of the ground acceleration is called Arias intensity (I_{A}), which is

$$I_{\mathrm{A}} = \frac{\pi}{2g}\int_0^T a^2(t)dt, \tag{13}$$

where g is the gravity acceleration, $a(t)$ is ground acceleration time history, and T is the entire duration of the ground motion record. D_{a5-75} is one of the common types of the signification duration [33], which is the time interval between 5% and 75% of I_{A} and is employed in this study.

Here, the calculation time is defined as $[t_1, t_2]$, where t_1 is the moment arriving at 5% of I_{A} and t_2 is the moment arriving at 75% of I_{A}. The additional EDR in the duration can be derived as follows:

$$\overline{\xi}_{\mathrm{a,peak}} = \xi_0 \frac{\int_{t_1}^{t_2} f_{\mathrm{d}}\dot{x}\,dt}{\int_{t_1}^{t_2} c\dot{x}^2 dt} = \xi_0 \frac{\int_0^{t_2} f_{\mathrm{d}}\dot{x}\,dt - \int_0^{t_1} f_{\mathrm{d}}\dot{x}\,dt}{\int_0^{t_2} c\dot{x}^2 dt - \int_0^{t_1} c\dot{x}^2 dt}, \tag{14}$$

where $\overline{\xi}_{\mathrm{a,peak}}$ is the additional EDR of the dampers in the calculation time $[t_1, t_2]$.

Similarly, equation (12) can be modified to obtain the additional EDR for the MDOF system in $[t_1, t_2]$:

$$\overline{\xi}_{\mathrm{a,peak}} = \xi_0 \frac{\sum_{i=1}^{n_1}\sum_{j=1}^{m}\int_{t_1}^{t_2} f_{\mathrm{d}j,i}\dot{x}_i dt}{\sum_{i=1}^{n}\int_{t_1}^{t_2} c_i \dot{x}_i^2 dt} = \xi_0 \frac{\sum_{i=1}^{n_1}\sum_{j=1}^{m}\left(\int_0^{t_2} f_{\mathrm{d}j,i}\dot{x}\,dt - \int_0^{t_1} f_{\mathrm{d}j,i}\dot{x}\,dt\right)}{\sum_{i=1}^{n}\left(\int_0^{t_2} c_i \dot{x}^2 dt - \int_0^{t_1} c_i \dot{x}^2 dt\right)}. \tag{15}$$

2.4. Procedure. The procedure of the calculation method based on energy dissipation is as follows:

(1) Time history analysis: because the energy dissipation should be calculated during a certain period, this method is applicable only for time history analysis.

(2) Calculation of the energy dissipation: the energy dissipation of natural damping and the additional dampers can be calculated by obtaining the integrals of the energy in equation (8) for SDOF systems and in equation (12) for MDOF systems.

(3) Calculation of the additional EDR during the entire seismic motion duration: the time history of the additional EDR provided by the dampers can be obtained by equation (8) for SDOF systems and equation (12) for MDOF systems during the entire seismic motion duration $[0, t]$.

(4) Determination of the duration $[t_1, t_2]$: the duration covering the intensive ground motion should be determined. t_1 is the moment arriving at 5% of I_{A} and t_2 is the moment arriving at 75% of I_{A}.

(5) Calculation of the additional EDR in the duration $[t_1, t_2]$: the energy dissipation of natural damping and the additional dampers during the duration $[t_1, t_2]$ can be calculated by obtaining the integrals in equation (14) for SDOF systems and equation (15) for MDOF systems. Then, the additional EDR induced by the dampers can be obtained using equation (14) and equation (15) for SDOF and MDOF systems, respectively.

3. Feasibility of the Proposed Method

To verify the feasibility of the proposed method, three viscously damped SDOF systems with different natural periods are introduced. In addition, a comparison study is conducted between this method and the classic strain energy method.

3.1. SDOF Systems. The natural periods of the three SDOF systems are 0.5 s, 1.0 s, and 2.0 s, respectively. Their masses are all equal to 204 *t*, and the inherent damping ratio is 0.05. The stiffnesses of the three systems are 32214.4 kN/m, 8048.6 kN/m, and 2013.4 kN/m. A linear viscous damper is added to the three SDOF systems, respectively. The Maxwell model is employed to simulate the mechanical behavior of the damper. The damping coefficient of the damper is set as 250 kN/(m/s). The diagram of the SDOF

systems is the same as that shown in Figure 1. The theoretical values of the additional EDRs induced by the added damper are 0.049, 0.097, and 0.195 for the three SDOF systems, respectively, which can be calculated using the differential equation of motion of the SDOF system.

Three sinusoidal waves with different periods, an artificial ground motion AWX, and a natural ground motion NRX are selected for the time history analysis. The periods of the three sine waves are 0.5, 1, and 2 s. And the PGAs of all the excitations are 0.035 g. The normalized spectra of the AWX and NRX records are plotted in Figure 2. The information of NRX is shown in Table 1, in which RSN is the record sequence number in the PEER ground motion database.

3.2. Numerical Analysis. Because of the adoption of a linear viscous damper, equation (8) becomes

$$\overline{\xi}_{\mathrm{a}}(t) = \xi_0 \frac{\int_0^t f_{\mathrm{d}} \dot{x}\, dt}{\int_0^t c\dot{x}^2 dt} = \xi_0 \frac{\int_0^t c_{\mathrm{a}} \dot{x}^2 dt}{\int_0^t c\dot{x}^2 dt} = \xi_0 \frac{c_{\mathrm{a}}}{c} = \frac{c_{\mathrm{a}}}{2m\omega_{\mathrm{n}}}, \quad (16)$$

which indicates that when the SDOF system is determined, the variation in the additional EDR $\overline{\xi}_{\mathrm{a}}(t)$ is related to only the damping coefficient of the added damper c_{a}.

The time histories of the cumulative energy dissipated by the damper and inherent damping can be obtained from dynamic analysis. The additional EDR can be obtained using equation (8). The time histories of the cumulative energy of the SDOF system with the period equaling to 1.0 s are shown in Figure 3. The time histories of the additional EDR fluctuate in the first few seconds when the system is not in steady motion. After that, the values of the additional EDR tend to be stable. The values for all the ground motions are the same in this system, equaling 0.097.

The values of additional EDR of the three SDOF systems are listed in Table 2. The frequencies of the excitations do not affect the calculation results of the additional EDR. The results show the feasibility of the proposed method.

The additional EDRs are also calculated by the strain energy method for comparison, of which the results are listed in Table 2. The additional EDRs are calculated using equation (1). Given that the added damper is a linear viscous damper, the energy dissipation can be calculated by the formula for the area of an ellipse:

$$E_{\mathrm{D}} = \pi \cdot F_{\mathrm{d\,max}} \cdot \Delta_{\mathrm{d\,max}}, \quad (17)$$

where $F_{\mathrm{d\,max}}$ is the maximum output force of the damper in a cycle and $\Delta_{\mathrm{d\,max}}$ is the maximum deformation of the damper in a cycle.

In the strain energy method, because the periods of the sine waves are known, the additional EDR in each vibration cycle can be obtained for the three cases involving the sine waves. Figure 4 shows the variation in the additional EDR from the calculation results of the strain energy method for the SDOF system with the period equaling to 1.0 s. The hysteresis curve of the damper in this system under the sine wave with $T = 0.5$ s is shown in Figure 4(d); the curve indicates that the energy dissipation capacity of the damper is fully utilized.

It can be observed from Table 2 that only when the system is in resonance, the result of the additional EDR in this case is consistent with the result obtained from structural dynamics [20]. In the other cases, because the ratio of the excitation frequency to the structural natural frequency causes errors in the strain energy method, the results of the additional EDR are not an accurate reflection of the energy dissipation capacity of the damper.

The comparison study between the proposed method and strain energy method shows that the proposed method not only is an easier approach to obtain the additional EDR but also provides calculation results that are more stable. This method can avoid the influence of the excitation frequency on the calculation result, which is a major problem of the strain energy method.

4. Example Illustration

4.1. Basic Information. A benchmark reinforcement concrete model is used to illustrate the usefulness of this method in practical engineering applications [34]. According to the Chinese code for the seismic design of buildings [22], the design PGA for dynamic analysis is 0.2 g and the characteristic period of the site soil is 0.4 s. The structural plan and elevation are depicted in Figure 5, and the dimensions of the cross sections of the members are listed in Table 3. The model of the structure is created using the software SAP2000 [35]. The beams and columns are modeled as elastic bars with plastic hinges at the two ends. The mechanical model of the hinges is the ideal rigid-plastic model, and the types of plastic hinges are moment M3 for the beams and interacting P-M2-M3 for the columns. The material of the members is reinforced concrete, and the design strength of the concrete is 30 MPa according to the code for the design of concrete structures [36]. The thin shell element is employed to simulate the floor slabs. The thickness of all the floors is set to be 0 mm so as to achieve optimal load transmission. The floors are subjected to distributed loads. The distributed dead loads are 5.5 kN/m^2, including the self-weight of the floor, for all the stories. The live loads are 3.0 kN/m^2 for stories 1–5 and 5.0 kN/m^2 for story 6. The story heights and loads are listed in Table 4. The Rayleigh damping is adopted in the structural model for dynamic analysis. The damping ratio is set to be 0.05 for the reinforcement concrete structure for the first and the fourth modes.

Two MYDs are installed at each story along the axes X3 and X7. The damper parameters are listed in Table 5. The damper installation diagram is also shown in Figure 5.

Next, nonlinear dynamic analysis is performed. To comply with the specifications of the Chinese code [22], seven earthquake ground motions are selected, of which five are natural ground motions. The natural ground motions are selected from the ground motion database of the Pacific Earthquake Engineering Research Center; the spectra of these ground motions are matched with the design acceleration spectrum [37]. The artificial ground motions are generated using a trigonometric method [38] and adjusted to

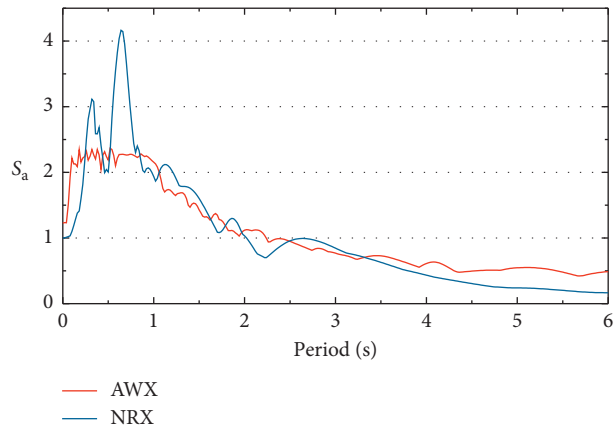

Figure 2: Normalized spectra of AWX and NRX.

Table 1: Information of NRX.

Name	RSN	Year	Magnitude	Resource	Station	t_1 (s)	t_2 (s)
NRX	760	1989	6.93	Loma Prieta	Foster City—Menhaden Court	5.79	13.055

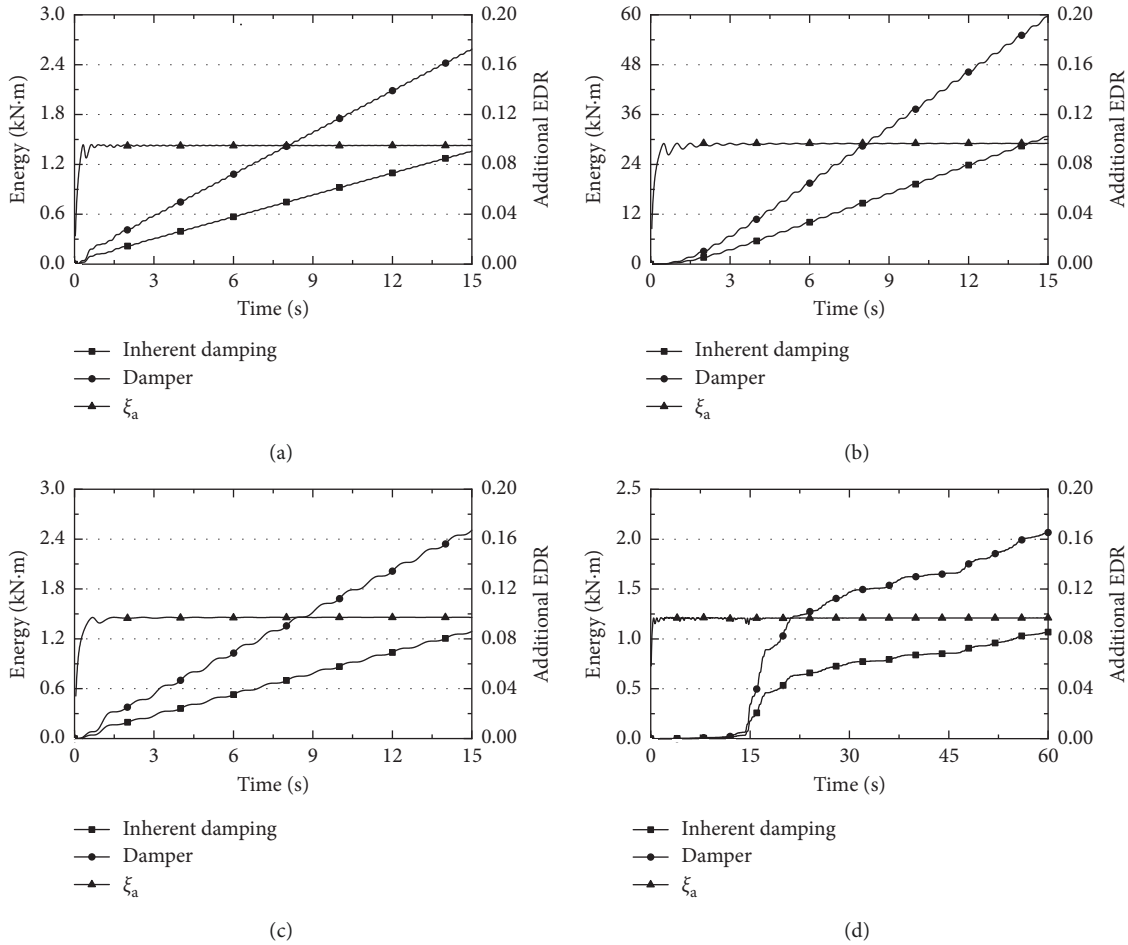

Figure 3: Continued.

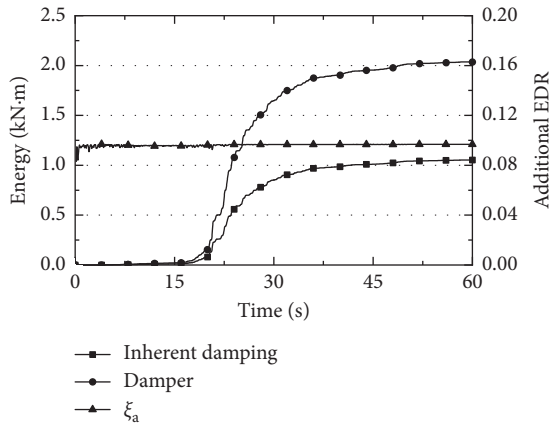

(e)

Figure 3: Cumulative energy dissipated by inherent damping and viscous damper and time histories of additional EDR of the SDOF system with the period equal to 1.0 s (the lines of inherent damping and the damper denote the cumulative energy dissipated by inherent damping and damper, respectively). (a) Sine wave, $T = 0.5$ s; (b) sine wave, $T = 1.0$ s; (c) sine wave, $T = 2.0$ s; (d) AWX; (e) NRX.

Table 2: Additional EDRs obtained by the strain energy method and proposed method for different cases.

Case	Strain energy method			Proposed method based on energy dissipation		
	$T_n = 0.5$ s	$T_n = 1.0$ s	$T_n = 2.0$ s	$T_n = 0.5$ s	$T_n = 1.0$ s	$T_n = 2.0$ s
$T = 0.5$ s	0.048	0.193	0.774	0.048	0.096	0.192
$T = 1.0$ s	0.024	0.097	0.389	0.048	0.097	0.194
$T = 2.0$ s	0.012	0.049	0.195	0.049	0.097	0.195
AWX	0.046	0.084	0.240	0.048	0.097	0.194
NRX	0.037	0.087	0.244	0.048	0.097	0.195

Note. T_n stands for the natural period of the SDOF systems, and T stands for the period of excitation period of the sine waves.

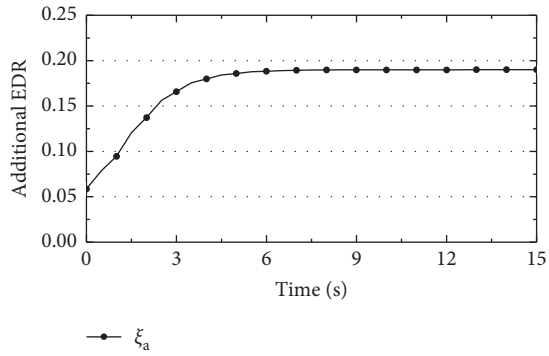

(a)

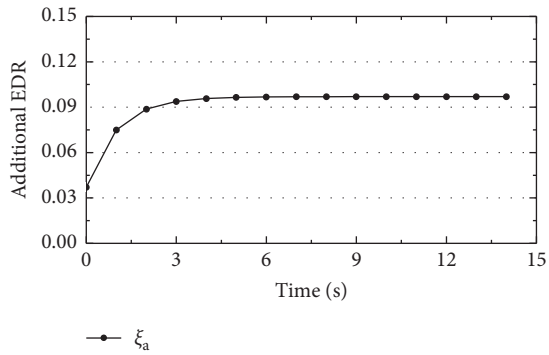

(b)

Figure 4: Continued.

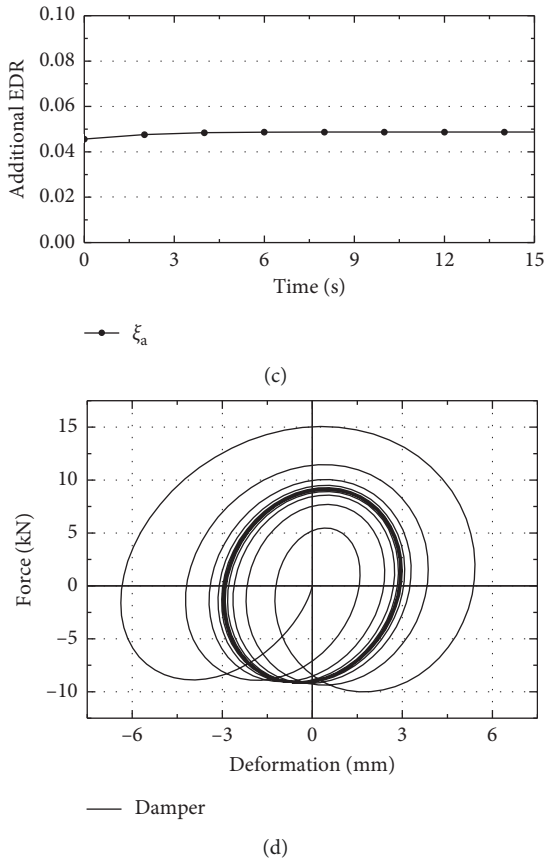

Figure 4: Time histories of additional EDRs obtained by the strain energy method under different sine waves of the SDOF system with the period equal to 1.0 s and hysteresis curve of the viscous damper for the system under the sine wave with $T = 0.5$ s. (a) Sine wave, $T = 0.5$ s; (b) sine wave, $T = 1.0$ s; (c) sine wave, $T = 2.0$ s; (d) hysteresis curve of damper.

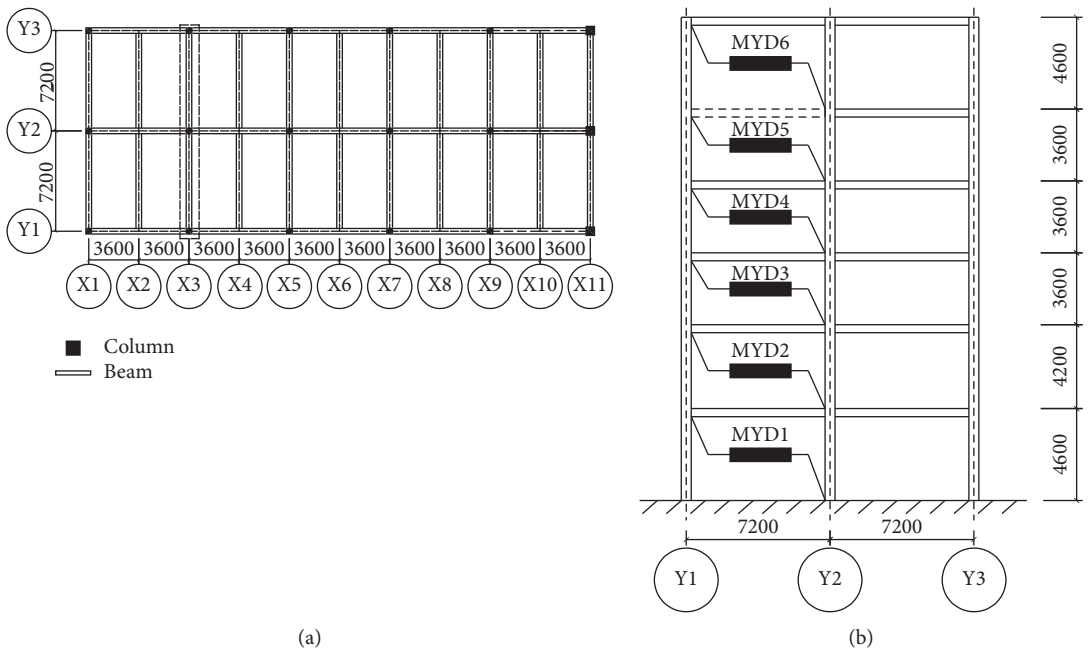

Figure 5: Structural plan and elevation (MYDs are installed in the Y direction) (unit: m): (a) Structural plan; (b) structural elevation.

Table 3: Dimensions of member cross sections.

	Story		
	1 and 2	3 and 4	5 and 6
Beam	350 mm × 600 mm	350 mm × 600 mm	350 mm × 600 mm
Column	700 mm × 700 mm	600 mm × 600 mm	500 mm × 500 mm

Table 4: Story heights and loads.

Story	Height (m)	Dead load (kN/m^2)	Live load (kN/m^2)
1	4.6	5.5	3.0
2	4.2	5.5	3.0
3	3.6	5.5	3.0
4	3.6	5.5	3.0
5	3.6	5.5	3.0
6	4.6	5.5	5.0

Table 5: Parameters of dampers at each story.

Story	Initial stiffness K_{I} (kN/m)	Yielding deformation $\Delta_{\mathrm{d}y}$ (mm)	Postyielding stiffness ratio α_{d}
1	1800	1	0.02
2	1800	1	0.02
3	1500	1	0.02
4	1500	1	0.02
5	1200	1	0.02
6	600	1	0.02

match the design response spectrum [39, 40]. For each earthquake, t_1 and t_2 are determined according to the definitions in Section 2.3. The details of the ground motions are listed in Table 6, and the normalized spectra of these ground motions are shown in Figure 6. The PGAs of the ground motions are set to 0.2 g.

4.2. Additional EDR Calculation. According to the proposed method, the additional EDR for the entire earthquake duration $[0, t]$ and $[t_1, t_2]$ is obtained using equations (12) and (15). In these two equations, the energy dissipated by inherent damping and the added dampers can be retrieved from the results of dynamic analysis in SAP2000. As a result, the time histories of ξ_{a} and the energy dissipated by natural damping and the MYDs can be easily obtained, which are shown in Figure 7.

For multistory structures, unlike the SDOF system, the time histories of additional EDR does not keep in a stable value, which fluctuate with the time throughout the duration of entire seismic motions. It can be observed that, after t_1, the inherent damping and the additional dampers started to dissipate the input energy and additional EDR increases sharply in the same time. And the energy dissipation of the dampers almost stops, and the fluctuation of the additional EDR tends to be gentle after the time t_2. It indicates that the dampers are fully utilized within the significant duration of ground motions.

Because of the difference of the frequency component and the duration of the ground motions, the responses of the structure, which are influenced by the higher modes, will be different. Moreover, except for the linear viscous dampers, the additional EDR induced by dampers are closely related to the amplitude of structural response [31], which results in the fluctuation of the time histories of additional EDR and the slight difference in the values of additional EDR obtained from different excitations.

Next, the strain energy method is adopted to calculate the additional EDR induced by the MYDs using equation (1). In the equation, the dissipated energy E_{D} and maximum strain energy E_{So} in one cycle are calculated as follows:

$$E_{\mathrm{D}} = 4 \cdot \sum_{j=1}^{M} K_{\mathrm{I}j} \cdot \Delta_{\mathrm{d}yj}^2 \cdot \left(1 - \alpha_{\mathrm{d}j}\right)\left(\mu_{\mathrm{d}j} - 1\right), \tag{18}$$

$$E_{\mathrm{So}} = \frac{1}{2} \sum_{i=1}^{N} Q_i \cdot \Delta_i + \frac{1}{2} \sum_{j}^{M} K_{\mathrm{I}j} \cdot \Delta_{\mathrm{d}yj}^2 \cdot \mu_{\mathrm{d}j} \cdot \left(1 + \mu_{\mathrm{d}j} \cdot \alpha_{\mathrm{d}j} - \alpha_{\mathrm{d}j}\right), \tag{19}$$

where $K_{\mathrm{I}j}$ denotes the initial stiffness of the j-th damper, $\Delta_{\mathrm{d}yj}$ denotes the yielding deformation of the j-th damper, $\alpha_{\mathrm{d}j}$ denotes the postyielding stiffness ratio of the j-th damper, and $\mu_{\mathrm{d}j}$ denotes the ductility factor of the j-th damper. Here, $\mu_{\mathrm{d}j} = \Delta_{\mathrm{d}j}/\Delta_{\mathrm{d}yj}$, where $\Delta_{\mathrm{d}j}$ denotes the deformation of the j-th damper, Q_i denotes the shear force at level i, Δ_i denotes the interstory displacement between level i and level i-1, M denotes the number of dampers, and N denotes the number of stories. Figure 8 shows the hysteresis curves of the MYDs at levels 1, 3, and 5 under the seismic motion AW1. The curves indicate that the energy dissipation capacity of the MYDs is fully utilized. The values obtained from equations (12), (15), and (1) are listed in Table 7.

Table 6: Details of input ground motion records.

Name	RSN	Year	Magnitude	Resource	Station	t_1 (s)	t_2 (s)
NW1	1768	1999	7.13	Hector Mine	Barstow	9.56	19.52
NW2	1838	1999	7.13	Hector Mine	Whitewater Trout Farm	6.36	16.38
NW3	4489	1999	6.3	L'Aquila, Italy	Montereale	9.34	23.44
NW4	6896	1999	7	Darfield, New Zealand	DORC	7.28	14.08
NW5	167	1999	6.53	Imperial Valley-06	Compuertas	15.24	31.36
AW1		—	—	—	—	5.9	20.58
AW2		—	—	—	—	6.42	22.4

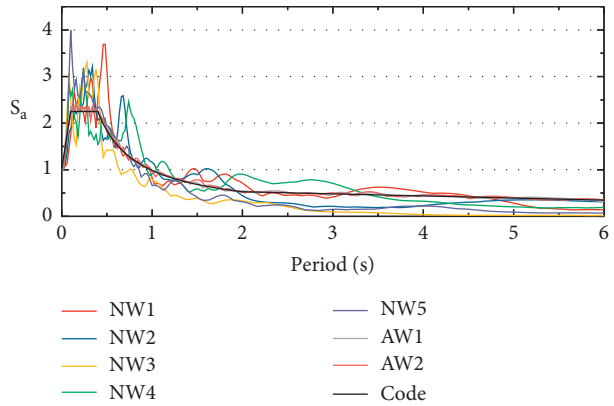

Figure 6: Spectra of normalized input ground motion records.

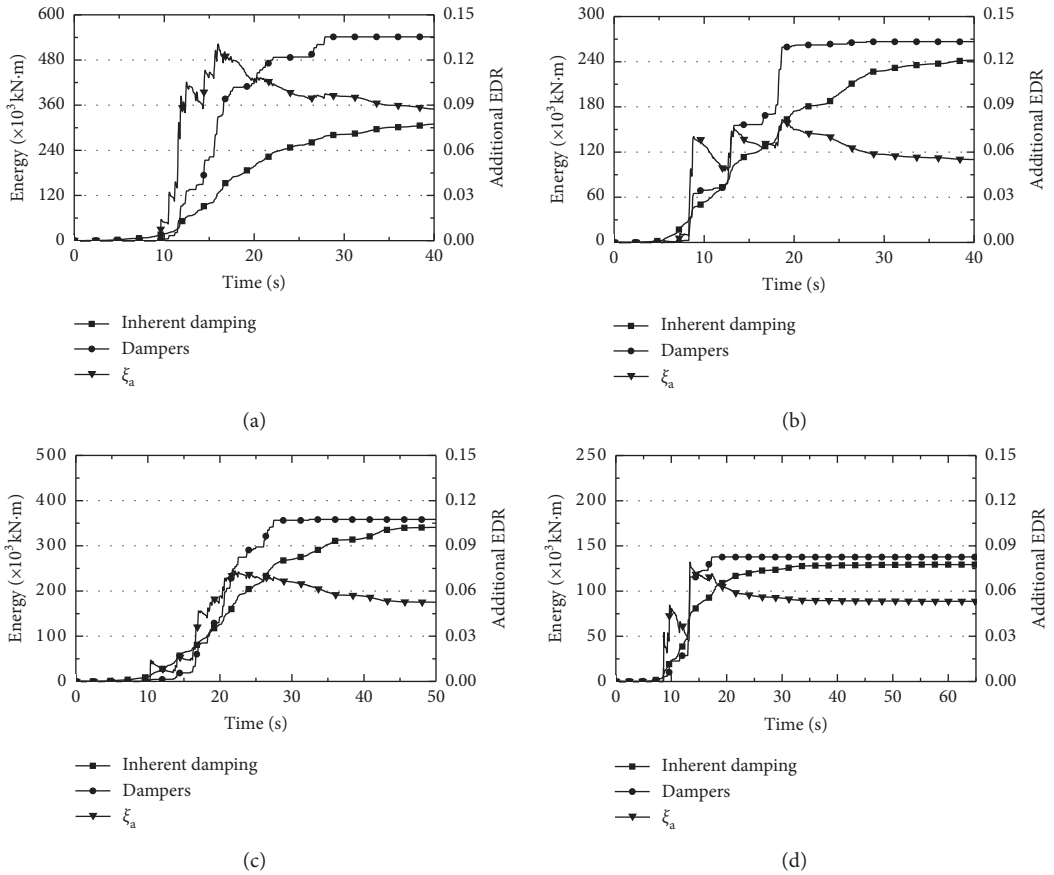

Figure 7: Continued.

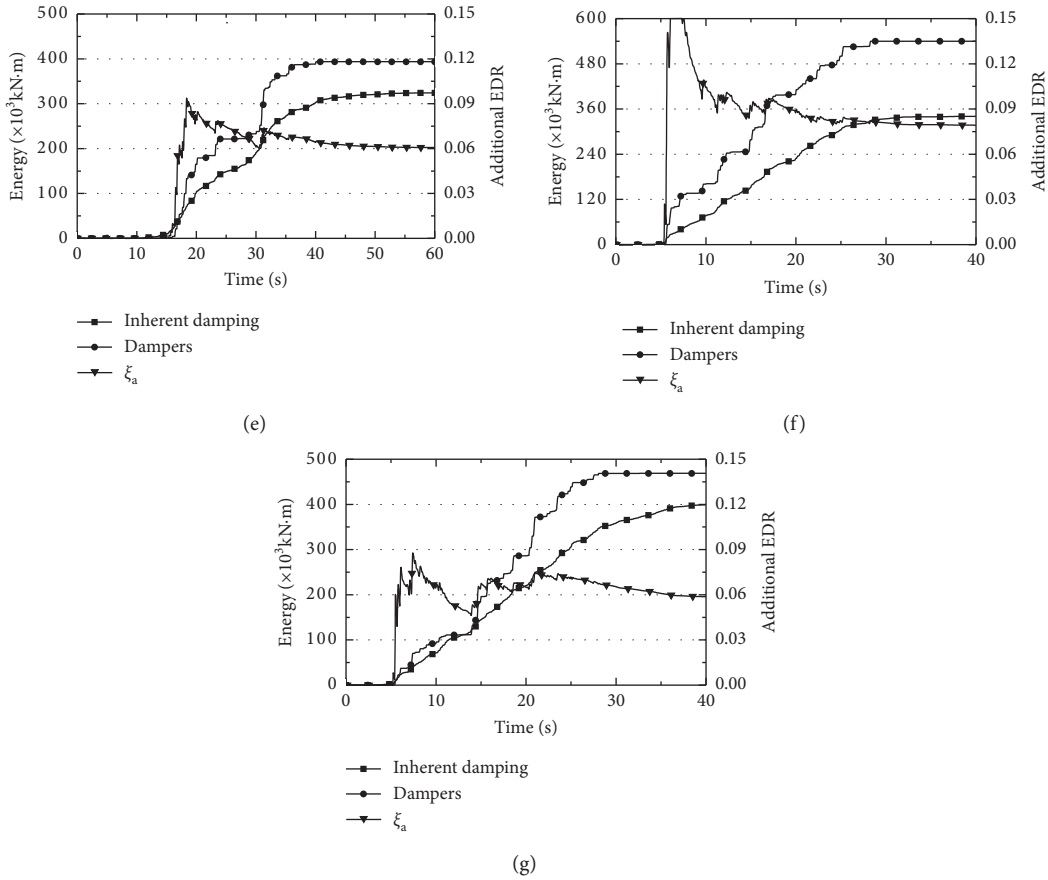

Figure 7: Cumulative energy dissipated by inherent damping and MYDs and time histories of additional EDR (the lines of inherent damping and the damper denote the cumulative energy dissipated by inherent damping and damper, respectively): (a) NW1; (b) NW2; (c) NW3; (d) NW4; (e) NW5; (f) AW1; (g) AW2.

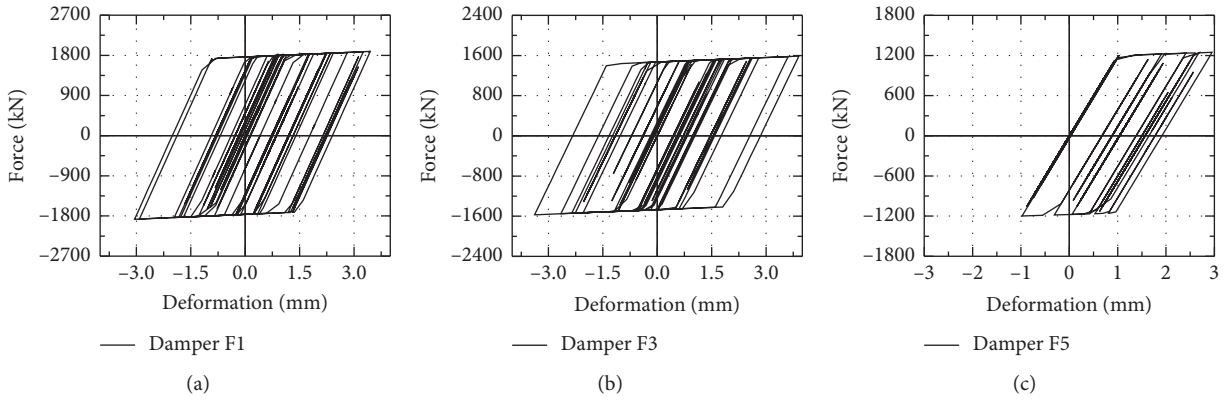

Figure 8: Hysteresis curves of MYDs under AW1: (a) damper at story 1; (b) damper at story 3; (c) damper at story 5.

4.3. Comparative Analysis. The responses of the structures with the additional EDR obtained from different methods (ST-end, ST-peak, and ST-strain) are compared with the response of the original structure (ST-original) to determine whether the results of the additional EDR can reflect the energy dissipation capacity of the MYDs. ST-end denotes the structure with $\xi_{a,end}$, ST-peak denotes the structure with $\xi_{a,peak}$, and ST-strain denotes the structure with $\xi_{a,strain}$. In these structures, the energy dissipation capacity of the MYDs is represented by the additional EDR obtained from different approaches and the Rayleigh damping are also adopted in these structures, of which the values are $0.05 + \xi_a$ for the first and fourth modes. The MYDs are modeled as elastic bars with equivalent stiffness, which can be calculated as follows [21]:

$$k_{j,\text{eff}} = \frac{F_{\text{d}j\max} - F_{\text{d}j\min}}{\Delta_{\text{d}j\max} - \Delta_{\text{d}j\min}}, \tag{20}$$

Table 7: Additional EDRs obtained by different approaches.

Case	$\xi_{a,end}$	$\xi_{a,peak}$	$\xi_{a,strain}$
NW1	0.085	0.118	0.213
NW2	0.055	0.068	0.185
NW3	0.053	0.074	0.204
NW4	0.053	0.075	0.170
NW5	0.061	0.078	0.184
AW1	0.079	0.083	0.210
AW2	0.059	0.073	0.201
Average	0.063	0.081	0.195

Note: $\xi_{a,end}$ is the final value of $\bar{\xi}_a$, $\xi_{a,peak}$ is the additional EDR induced by the dampers during the duration $[t_1, t_2]$, and $\xi_{a,strain}$ is the value obtained from the strain energy method.

where $k_{j,eff}$ denotes the equivalent stiffness of the j-th damper; $F_{dj\max}$ and $F_{dj\min}$ denote the maximum and minimum damping forces of the j-th damper, respectively, under a certain earthquake; and $\Delta_{j\max}$ and $\Delta_{j\min}$ denote the maximum and minimum deformations of the j-th damper, respectively, under a certain earthquake. Here, $k_{j,eff}$ is the average of the equivalent stiffnesses under the seven seismic ground motions.

Next, the dynamic analysis is carried out. The story shears and story drifts of the three structures are compared with that of the original structure, as shown in Figures 9 and 10, respectively.

The above comparison clearly indicates that all the responses are close. The response of ST-peak is closest to that of ST-original. The response of ST-end is larger than that of ST-original, whereas the response of ST-strain is smaller than that of ST-original. Because the response of ST-end is larger than that of ST-original, the value of $\zeta_{a,end}$ is small. Generally, during most of the entire earthquake duration, the seismic responses of the structures are considerably smaller than the maximum responses of the structures. Therefore, the MYDs are not always utilizing their maximum capacity during the entire seismic duration. The energy dissipation capacity of the dampers can be underestimated within the entire earthquake duration. Therefore, the additional EDR is estimated during the most intensive period in the entire seismic motion duration.

The responses of ST-strain are smaller than those of ST-original, which means that $\xi_{a,strain}$ is too large. Currently, the strain energy method is the most common approach used to estimate the additional EDR. However, for practical applications, the method not only is complicated in terms of calculation but also overestimates the additional EDR in some cases. In the example considered in this study, the error in $\xi_{a,strain}$ may be attributed to the following causes:

(1) The seismic motion is a stochastic process, which can be represented by a combination of a series of sine waves with a wide range of frequencies. As discussed in Section 3.2, the frequency of the excitation will cause obvious errors in the results of the additional EDR obtained by the strain energy method.

(2) The energy dissipation is obtained according to the maximum deformations of the dampers based on equation (18). However, the maximum deformations of the dampers in different levels usually do not occur at the same time during the vibration. The sum of the energy dissipation values of the dampers based on the maximum deformations during the entire earthquake will overestimate the mitigation effect of the MYDs.

(3) The strain energy method is derived using an elastic SDOF system. When the primary structure is driven into the inelastic range, the method can cause obvious errors in the calculation of the strain energy and dissipated energy; hence, the calculation equations for these energies should be modified.

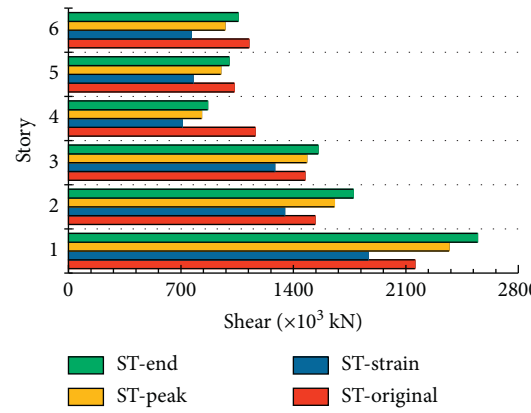

Figure 9: Story shears.

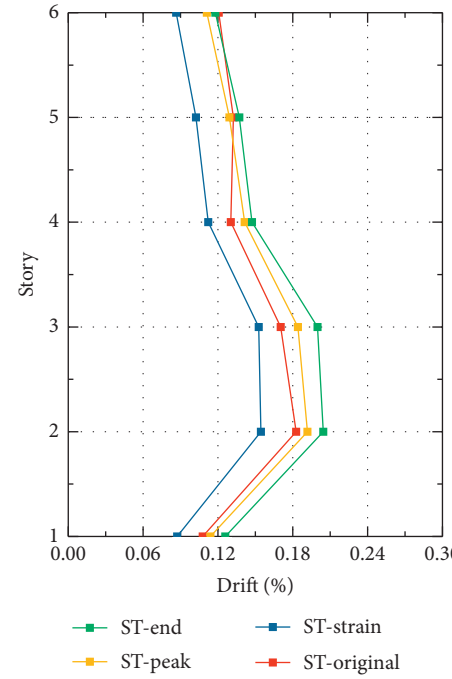

Figure 10: Story drifts.

5. Conclusion

In this paper, a simple method is proposed for the fast estimation of the additional EDR of damped structures. The

method is derived from the definition of the EDR in structural dynamics. Through time history analysis, the ratio of the energy consumption of inherent damping to that of the added dampers can be obtained under external excitation. The additional EDR can be estimated using the inherent damping ratio and energy consumption ratio. Based on the study results, the following conclusions can be drawn:

(1) The concept of the method is explicit, intuitive, and easy to understand for structural practitioners. By using the inherent damping ratio and the ratio of the energy dissipated by dampers to that dissipated by inherent damping, the additional EDR can be accurately estimated.

(2) Unlike the strain energy method, the proposed method can eliminate the influence of the excitation frequency on the result of the additional EDR, which means that the additional EDR obtained by this method is a better reflection of the energy dissipation capacity of dampers.

(3) The time-varying characteristic of the additional EDR is revealed in this study. Except for the linear viscous dampers, the additional EDR induced by the dampers in the structure is not constant and fluctuates in the duration of ground motions. To improve the accuracy, the estimation of additional EDR should be calculated within the significant duration of ground motion.

(4) The proposed method focuses on the energy dissipation of inherent damping and the dampers and hence is not related to the state of the structure. Therefore, this method is applicable to not only elastic structures but also structures in the inelastic state.

Data Availability

The data used to support the findings of this study are available from the corresponding author upon request.

Conflicts of Interest

The authors declare that they have no conflicts of interest.

Acknowledgments

This study was supported by the Shanghai Pujiang Program under Grant no. 17PJ1409200 and the Fundamental Research Funds for the Central Universities under Grant no. 22120180064.

References

[1] B. Basu, O. S. Bursi, F. Casciati et al., "A european association for the control of structures joint perspective. Recent studies in civil structural control across europe," *Structural Control and Health Monitoring*, vol. 21, no. 12, pp. 1414–1436, 2014.

[2] K. Ghaedi, Z. Ibrahim, H. Adeli, and A. Javanmardi, "Invited review: recent developments in vibration control of building and bridge structures," *Journal of Vibroengineering*, vol. 19, no. 5, pp. 3564–3580, 2017.

[3] T. T. Song and G. F. Dargush, *Passive Energy Dissipation Systems in Structural Engineering*, John Wiley & Sons, New York, NY, USA, 1998.

[4] C. Pan, R. Zhang, H. Luo, C. Li, and H. Shen, "Demand-based optimal design of oscillator with parallel-layout viscous inerter damper," *Structural Control and Health Monitoring*, vol. 25, no. 1, article e2051, 2018.

[5] W.-H. Lin and A. K. Chopra, "Earthquake response of elastic sdf systems with non-linear fluid viscous dampers," *Earthquake Engineering & Structural Dynamics*, vol. 31, no. 9, pp. 1623–1642, 2002.

[6] F. Mazza, "Nonlinear seismic analysis of unsymmetric-plan structures retrofitted by hysteretic damped braces," *Bulletin of Earthquake Engineering*, vol. 14, no. 4, pp. 1311–1331, 2016.

[7] A. M. Avossa and G. Pianese, "Damping effects on the seismic response of base-isolated structures with LRB devices," *Ingegneria Sismica*, vol. 34, pp. 3–29, 2017.

[8] R. Zhang, C. Wang, C. Pan, H. Shen, Q. Ge, and L. Zhang, "Simplified design of elastoplastic structures with metallic yielding dampers based on the concept of uniform damping ratio," *Engineering Structures*, vol. 176, pp. 734–745, 2018.

[9] F. Sadek, B. Mohraz, and M. A. Riley, "Linear procedures for structures with velocity-dependent dampers," *Journal of Structural Engineering*, vol. 126, no. 8, pp. 887–895, 2000.

[10] O. M. Ramirez, M. C. Constantinou, A. S. Whittaker, C. A. Kircher, M. W. Johnson, and C. Z. Chrysostomou, "Validation of the 2000 NEHRP provisions' equivalent lateral force and modal analysis procedures for buildings with damping systems," *Earthquake Spectra*, vol. 19, no. 4, pp. 981–999, 2003.

[11] J. P. D. Hartog, *Mechanical Vibrations*, McGraw-Hill, New York, NY, USA, 4th edition, 1956.

[12] K. C. Chang, M. L. Lai, T. T. Soong, D. S. Hao, and Y. C. Yeh, "Seismic behavior and design guidelines for steel frame structures with added viscoelastic dampers," in *Technical Report NCEER-93-0009*, National Center for Earthquake Engineering Research, Buffalo, NY, USA, 1993.

[13] Y. Y. Lin, M. H. Tsai, J. S. Hwang, and K. C. Chang, "Direct displacement-based design for building with passive energy dissipation systems," *Engineering Structures*, vol. 25, no. 1, pp. 25–37, 2003.

[14] J. W. W. Guo and C. Christopoulos, "Performance spectra based method for the seismic design of structures equipped with passive supplemental damping systems," *Earthquake Engineering & Structural Dynamics*, vol. 42, no. 6, pp. 935–952, 2013.

[15] L. Landi, S. Lucchi, and P. P. Diotallevi, "A procedure for the direct determination of the required supplemental damping for the seismic retrofit with viscous dampers," *Engineering Structures*, vol. 71, pp. 137–149, 2014.

[16] L. Hao and R. Zhang, "Structural safety redundancy-based design method for structure with viscous dampers," *Structural Engineering and Mechanics*, vol. 59, no. 5, pp. 821–840, 2016.

[17] S. Wang and S. A. Mahin, "High-performance computer-aided optimization of viscous dampers for improving the seismic performance of a tall building," *Soil Dynamics and Earthquake Engineering*, vol. 113, pp. 454–461, 2018.

[18] G. A. Papagiannopoulos and G. D. Hatzigeorgiou, "On the use of the half-power bandwidth method to estimate damping in building structures," *Soil Dynamics and Earthquake Engineering*, vol. 31, no. 7, pp. 1075–1079, 2011.

[19] J.-T. Wang, F. Jin, and C.-H. Zhang, "Estimation error of the half-power bandwidth method in identifying damping for multi-DOF systems," *Soil Dynamics and Earthquake Engineering*, vol. 39, pp. 138–142, 2012.

[20] A. K. Chopra, *Dynamics of Structures: Theory and Applications to Earthquake Engineering*, Prentice hall, Upper Saddle River, NJ, USA, 4th edition, 2012.

[21] American Society of Civil Engineers, *FEMA356 Prestandard and Commentary for the Seismic Rehabilitation of Buildings: Rehabilitation Requirements*, pp. 9–30, American Society of Civil Engineers, Washington, DC, USA, 2000.

[22] China Architecture & Building Press, *Chinese Code for Seismic Design of Buildings (GB50011-2010)*, China Architecture & Building Press, Beijing, China, 2010.

[23] S.-H. Lee, K.-W. Min, J.-S. Hwang, and J. Kim, "Evaluation of equivalent damping ratio of a structure with added dampers," *Engineering Structures*, vol. 26, no. 3, pp. 335–346, 2004.

[24] A. Occhiuzzi, "Additional viscous dampers for civil structures: analysis of design methods based on effective evaluation of modal damping ratios," *Engineering Structures*, vol. 31, no. 5, pp. 1093–1101, 2009.

[25] P. P. Diotallevi, L. Landi, and A. Dellavalle, "A methodology for the direct assessment of the damping ratio of structures equipped with nonlinear viscous dampers," *Journal of Earthquake Engineering*, vol. 16, no. 3, pp. 350–373, 2012.

[26] J.-H. Park, "Seismic response of SDOF systems representing masonry-infilled RC frames with damping systems," *Engineering Structures*, vol. 56, pp. 1735–1750, 2013.

[27] H. Guerrero, J. A. Escobar, and A. Teran-Gilmore, "Experimental damping on frame structures equipped with buckling-restrained braces (BRBs) working within their linear-elastic response," *Soil Dynamics and Earthquake Engineering*, vol. 106, pp. 196–203, 2018.

[28] G. A. Papagiannopoulos and D. E. Beskos, "On a modal damping identification model for non-classically damped linear building structures subjected to earthquakes," *Soil Dynamics and Earthquake Engineering*, vol. 29, no. 3, pp. 583–589, 2009.

[29] P. S. Katsimpini, G. A. Papagiannopoulos, and M. G. Sfakianakis, "On the seismic response and damping capacity of low-rise plane steel frames with seesaw system," *Soil Dynamics and Earthquake Engineering*, vol. 107, pp. 407–416, 2018.

[30] C. Li, T. Li, D. Ban, and X. Ge, "Equivalent damping of SDOF structure with Maxwell damper," *Earthquake Engineering and Engineering Vibration*, vol. 17, no. 3, pp. 627–639, 2018.

[31] R. W. Clough and J. Penzien, *Dynamics of Structures*, Computers & Structures, Inc., Berkeley, CA, USA, 3rd edition, 2003.

[32] J. J. Bommer and A. Martínez-pereira, "The effective duration of earthquake strong motion," *Journal of Earthquake Engineering*, vol. 3, no. 2, pp. 127–172, 1999.

[33] J. J. Kempton and J. P. Stewart, "Prediction equations for significant duration of earthquake ground motions considering site and near-source effects," *Earthquake Spectra*, vol. 22, no. 4, pp. 985–1013, 2006.

[34] D. G. Weng, R. F. Zhang, S. M. Zhang, and X. L. Lu, "Application of energy dissipation method based on seismic performance and demand for post-earthquake R.C. frame retrofit," in *Proceeding of the 11th World Conference on Seismic Isolation, Energy Dissipation and Active Vibration Control of Structure*, Guangzhou, China, 2009.

[35] E. L. Wilson, *SAP2000: Integrated Finite Element Analysis Design of Structures*, Computers and Structures, Inc, Berkeley, CA, USA, 1997.

[36] China Architecture & Building Press, *Code for Design of Concrete Structures (GB50010-2010)*, China Architecture & Building Press, Beijing, China, 2010.

[37] B. Darragh, W. Silva, and N. Gregor, "Strong motion record processing procedures for the PEER center," in *Proceedings of the COSMOS Workshop on Strong-Motion Record Processing*, pp. 1–12, Richmond, CA, USA, May 2004.

[38] Y. Bozorgnia and V. V. Bertero, *Earthquake Engineering: From Engineering Seismology to Performance-Based Engineering*, CRC Press, Boca Raton, FL, USA, 2004.

[39] C. Pan, R. Zhang, H. Luo, and H. Shen, "Baseline correction of vibration acceleration signals with inconsistent initial velocity and displacement," *Advances in Mechanical Engineering*, vol. 8, no. 10, article 168781401667553, 2016.

[40] C. Pan, R. Zhang, H. Luo, and H. Shen, "Target-based algorithm for baseline correction of inconsistent vibration signals," *Journal of Vibration and Control*, vol. 24, no. 12, pp. 2562–2575, 2017.